PHYSICAL REVIEW B VOLUME 17, NUMBER 6 15 MARCH 1978

Surfaces of real metals by the variational self-consistent method

R. Monnier*†
NORDITA, Blegdamsvej 17, DK-2100 Copenhagen, Denmark

J. P. Perdew‡§
Department of Physics, Rutgers University, New Brunswick, New Jersey 08903
(Received 7 July 1977)

We present a self-consistent calculation of the ground state of the metallic planar surface in which the discrete-lattice perturbation $\delta v(\vec{r})$ is treated variationally, with use of a single variational parameter, rather than perturbatively. Our calculation, which reduces to the perturbation theory of Lang and Kohn in the limit of weak $\delta v(\vec{r})$ and retains most of the simplicity and broad utility of their approach, shows that for many metal surfaces $\delta v(\vec{r})$ is *not* a weak perturbation: The electron density profiles at real metal surfaces are often unlike those of the jellium model and in fact show a strong dependence on the choice of exposed crystallographic face. This face dependence, which is rather simply related to the average value $\langle \delta v \rangle_{av}$ of the discrete-lattice perturbation over the volume of the semi-infinite crystal may have important consequences in the calculation of many surface-related properties, including chemisorption, to which our method is easily applicable. We calculate the face-dependent surface energies, density profiles, and work functions of nine simple metals. Calculated surface energies, including the correction to the local-density approximation for exchange and correlation given by the method of wave-vector analysis, are in good agreement with measured surface tensions for those seven of the nine metals in which the ionic pseudopotential gives a good account of the *bulk* binding energy. Problems still to be considered include improvements in the pseudopotential, lattice relaxation at the surface, and variation of the electron density over planes parallel to the surface.

I. INTRODUCTION

We present a *variational self-consistent* treatment of the ground state of the metal surface, with numerical results for the face-dependent electron density profiles, surface energies, and work functions of nine simple metals. A preliminary report of our work, with surface energies for the most densely packed faces of the cubic metals, has already appeared.[1] Our method, which is a direct generalization of the Lang-Kohn *perturbational self-consistent method*,[2] combines the computational simplicity (e.g., electron density variation only in the direction normal to the surface) and broad utility of the latter with features that might otherwise be found only in complicated three-dimensional self-consistent calculations. Our results show that (i) the surface energies for *some* metal surfaces are significantly lower than the values predicted by the perturbational self-consistent method, and (ii) the electron density profiles for *most* metal surfaces are significantly different from the semi-infinite jellium-model profiles used in the perturbational self-consistent method, and in fact depend strongly on the exposed crystallographic face. Point (ii) may have important consequences in calculations of surface-related properties such as chemisorption and adhesion, to which our method is easily applicable; in fact our method has already been applied to the calculation of vacancy-formation energies[3] and of the equilibrium position and binding energy of hydrogen chemisorbed on the (111) face of Al.[4] The work function calculations we shall present here are only intended to show that the weak face dependence[5] of the work function is compatible with, and in fact requires, a strong face dependence of the electron density profile; a more accurate calculation of face-dependent work functions will be given in a subsequent paper.[6]

We include the correction to the local density approximation for exchange and correlation given by the method of wave-vector analysis.[7-9] The surface energies so calculated for the most densely packed faces are in good agreement with measured liquid-metal surface tensions for those metals (Al, Pb, Mg, Na, K, Rb, and Cs) in which the pseudopotential also gives a good account of the *bulk* binding energy, and in poor agreement for Li and Zn in which the pseudopotential gives a poor description of the bulk (as discussed in Sec. II).

The advent of density functional theory[10, 11] permitted the first realistic treatment of the jellium model of the metal surface, in which the semi-infinite lattice of ions is replaced by a semi-infinite uniform positive background. Results of this work[2, 12, 13] showed that (a) exchange and correlation, usually treated in the local density approximation[11] (LDA), have a major effect on the electron density profile, work function, and surface energy, and (b) while the work functions of the jellium model agree (within about 15%) with the work functions of real metals, the jellium model fails for the surface energies, even to the extent

of giving the wrong or negative sign for the surface energies of the metals of higher electron density like Al. This effort culminated in the classical work of Lang and Kohn,[2] who gave a fully self-consistent treatment of the jellium model within the LDA. They then reintroduced $\delta v(\vec{r})$, the difference between the pseudopotentials of the semi-infinite lattice of ions and the electrostatic potential of the semi-infinite uniform positive background, as a first-order perturbation to the surface energies[2] and work functions.[5] Their results for the surface energies of the most densely packed faces and the face-dependent work functions showed reasonable agreement with the admittedly inadequate experimental values, the worst error being an overestimate of the surface energy of Pb by a factor of about 2.

The Lang-Kohn approach has an appealing and physically reasonable simplicity: all the complexities of the bulk band structure, which are known to have little effect on the bulk binding energy (see Sec. II), are simply ignored, and all the inhomogeneity left in the problem is the essential one-dimensional inhomogeneity of the surface itself. The self-consistency problem is easily solved for one-dimensional density variation (and the numerical instabilities that formerly precluded a straightforward iterative solution can now be eliminated by means of an integral equation for the electostatic potential; see Appendix A). The one-electron wave functions of the jellium model tend in the interior of the metal to phase-shifted free-electron waves,[2] and these phase shifts, which satisfy a charge-neutrality sum rule,[14, 15] can be used to express the surface kinetic energy,[2] the surface density of states,[16] and other one-electron properties.[17] Because of its relative conceptual and numerical simplicity, the Lang-Kohn-type approach has also been applied to other problems such as surface spin susceptibility,[18, 19] vacancy formation,[20] adhesion,[21,22] and chemisorption,[23, 24] and may prove useful for still others such as surface-plasmon dispersion. We have therefore chosen to retain all of these simplifying features in our variational self-consistent approach.

On the other hand, the Lang-Kohn treatment of $\delta v(\vec{r})$ as a weak first-order perturbation must be regarded with skepticism for most metal surfaces. As mentioned earlier, $\delta v(\vec{r})$ makes a very large contribution to the surface energy, especially in the denser metals like Al. A calculation by Finnis[25] suggests that second-order corrections can be very large in such metals.

Furthermore, $\langle \delta v \rangle_{\text{av}}$, the average value of $\delta v(\vec{r})$ over the volume of the semi-infinite crystal, is often a large fraction of both the free-electron Fermi energy and the one-electron potential barrier of the jellium surface. (Values of this face-dependent $\langle \delta v \rangle_{\text{av}}$ are given in Table I). This large *average* potential has no effect on the electron-density variation in the bulk, and so first-order perturbation theory in $\delta v(\vec{r})$ is appropriate for the bulk binding energy. However, since $\delta v(\vec{r})$ vanishes outside the metal and has a large average value inside, it is bound to have a significant effect on the electron-density variation at the surface. These facts suggested to us that $\delta v(\vec{r})$ should be treated variationally (or exactly) rather than perturbatively. We formulated the variational self-consistent method so that it would reduce exactly to the Lang-Kohn perturbational self-consistent method in the limit where $\delta v(\vec{r})$ becomes sufficiently weak. Our results show that for most surfaces $\delta v(\vec{r})$ is *not* weak enough to be treated as a first-order perturbation. We

TABLE I. Values of $\langle \delta v \rangle_{\text{av}}$, the average value of the discrete-lattice perturbation over the volume of the semi-infinite crystal. The crystallographic faces for each metal, labeled by their Miller indices, are arranged from the most to the least densely packed.

Metal	Face	$\langle \delta v \rangle_{\text{av}}$ (eV)	Metal	Face	$\langle \delta v \rangle_{\text{av}}$ (eV)
Al fcc	(111)	−1.7	Na bcc	(110)	0.0
	(100)	0.2		(100)	0.9
	(110)	3.0		(111)	1.5
Pb fcc	(111)	−3.9	K bcc	(110)	0.1
	(100)	−1.9		(100)	0.8
	(110)	1.2		(111)	1.3
Zn hcp	(0001)	−0.7	Rb bcc	(110)	0.6
Mg hcp	(0001)	−0.2		(100)	1.3
				(111)	1.7
Li bcc	(110)	−0.8	Cs bcc	(110)	0.7
	(100)	0.2		(100)	1.3
	(111)	0.9		(111)	1.8

have found that the difference of our density profiles from those of the jellium model correlates strongly with the sign and size of $\langle \delta v \rangle_{av}$, which is also an important ingredient of our expression for the work function.

Of course a complete description of the ground state of the metal surface requires the full solution of a three-dimensional self-consistent problem—the best-founded result of the variational self-consistent method is an upper bound on the surface energy, given the correct energy functional. To date such three-dimensional treatments exist for only a few of the simple metals and for selected faces: Al(111),[26,27] Al(110),[28] Al(100),[29,30] Li(100)[30,31], Na(100),[30,32] and Cs(100).[30] These calculations employ diverse treatments of the ionic pseudopotential and the exchange-correlation potential, and achieve varying degrees of self-consistency. In many of them the primary interest has been in selected surface and bulk states; in only a few of them is the electron-density profile displayed,[27,29,31,32] and surprisingly the surface energy is not determined in any of them.

Aside from these calculations, most recent theoretical work on the surface ground state involves a closer look at the jellium model: One line of investigation has been the introduction of corrections to the LDA by means of the density gradient expansion[33-35] or wave-vector analysis.[7-9] Another line has been the design of rather accurate variational or model-potential methods[36,37] which bypass the need for numerical iteration.

The first step toward a variational treatment of real metal surfaces was apparently taken by Paasch and Hietschold,[38,39] who used a direct parametrization of the electron-density profile. Their conclusions about the strong face dependence of the profile are in qualitative agreement with ours. (While Lang and Kohn have already given a systematic study of the face dependence of the work function,[5] their perturbative approach conceals the face-dependence of the profile). The work of Paasch and Hietschold also suggests that lattice relaxation at the surface, not considered here except in Appendix E, may be important for some metal surfaces, although some of their approximations appear too severe to be quantitatively reliable.

II. ENERGY FUNCTIONAL

The ground-state energy of a system of electrons interacting with static ions via a local pseudopotential can be written as a functional[10,11] of the electron number density $n(\vec{r})$

$$E[n] = T_s[n] + E_{xc}[n] + \frac{e^2}{2}\int d\vec{r}\, d\vec{r}\,' \frac{n(\vec{r})n(\vec{r}\,')}{|\vec{r}-\vec{r}\,'|} + \int d\vec{r} \sum_{\vec{l}} w(|\vec{r}-\vec{l}|)n(\vec{r}) + \frac{1}{2}\sum_{\vec{l},\vec{l}\,}{}' \frac{(ze)^2}{|\vec{l}-\vec{l}\,'|} . \tag{2.1}$$

The first three terms of (2.1) are the noninteracting kinetic energy, exchange-correlation energy, and Hartree electrostatic energy respectively, as defined in density functional theory.[10,11] The ionic pseudopotential w has a long-range attractive part and a short-range repulsive part w_R

$$w(r) = -\frac{ze^2}{r} + w_R(r) . \tag{2.2}$$

[$n(\vec{r})$ is strictly the pseudo electron density, but we do not bother to retain this cumbersome terminology.] The last term in (2.1) is the Coulomb interaction between the ions distributed over sites $\vec{l}$, and the prime means that the $\vec{l}\,' = \vec{l}$ term is omitted from the sum.

For large systems, where the individual Coulomb terms of (2.1) are badly behaved, it is convenient to add and subtract a fictitious neutralizing positive background $n_+(\vec{r})$ (defined later as that of the jellium model) to Eq. (2.1), with the result

$$E[n] = T_s[n] + E_{xc}[n] + \frac{1}{2}\int d\vec{r}\, \phi([n];\vec{r})[n(\vec{r}) - n_+(\vec{r})] + \int d\vec{r}\, \delta v(\vec{r})[n(\vec{r}) - n_+(\vec{r})] + \int d\vec{r} \sum_{\vec{l}} w_R(|\vec{r}-\vec{l}|)n_+(\vec{r}) + \left(\frac{1}{2}\int d\vec{r}\, d\vec{r}\,' \frac{n_+(\vec{r})n_+(\vec{r}\,')}{|\vec{r}-\vec{r}\,'|} - \int d\vec{r} \sum_{\vec{l}} \frac{ze^2}{|\vec{r}-\vec{l}|} n_+(\vec{r}) + \frac{1}{2}\sum_{\vec{l},\vec{l}\,}{}' \frac{(ze)^2}{|\vec{l}-\vec{l}\,'|}\right), \tag{2.3}$$

where[40]

$$\phi([n];\vec{r}) = e^2 \int d\vec{r}\,' \frac{n(\vec{r}\,') - n_+(\vec{r}\,')}{|\vec{r}-\vec{r}\,'|} \tag{2.4}$$

and

$$\delta v(\vec{r}) = \sum_{\vec{l}} w(|\vec{r}-\vec{l}|) + e^2 \int d\vec{r}\,' \frac{n_+(\vec{r}\,')}{|\vec{r}-\vec{r}\,'|} . \tag{2.5}$$

The auxiliary one-electron wave functions ψ_i of density functional theory,[11] which are used to con-

TABLE II. Calculated bulk binding energy ϵ and the exchange-correlation (ϵ_{xc}), first-order pseudopotential ($\bar{w}_R$), and band-structure (ϵ_{bs}) contributions to it. The kinetic energy ($\epsilon_s = \frac{3}{5}\epsilon_F(\bar{n})$) and Madelung ($\epsilon_M$) contributions are not shown. The alkali metals have been treated here as bcc and the others as fcc. ϵ^{exp} is the measured binding energy (from Ref. 41). The first-order [$\langle \delta v_{WS} \rangle_{av}$, Eq. (4.10)] and band-structure (μ_{bs}, see Appendix C) *bulk* contributions to the chemical potential are also shown.

Metal	$\epsilon_{xc}(\bar{n})$	$\bar{w}_R$	ϵ_{bs}	(eV) ϵ	ϵ^{exp}	$\langle \delta v_{WS} \rangle_{av}$	μ_{bs}
Al	−7.2	5.8	−0.0	−18.9	−18.8	−2.4	−0.0
Pb	−6.6	4.2	−0.5	−24.0	−24.3	−4.7	−0.2
Zn	−6.6	5.4	−0.3	−12.6	−14.3	−0.2	−0.2
Mg	−5.9	4.2	−0.1	−12.1	−12.1	−0.7	−0.1
Li	−4.9	1.3	−0.0	−8.2	−7.0	−1.2	−0.0
Na	−4.1	1.8	−0.1	−6.6	−6.3	−0.3	−0.1
K	−3.5	1.5	−0.1	−5.7	−5.3	−0.1	−0.1
Rb	−3.3	1.9	−0.3	−5.2	−5.0	0.4	−0.3
Cs	−3.1	2.0	−0.4	−4.9	−4.7	0.5	−0.4

struct $n(\vec{r})$ and $T_s[n]$, satisfy the self-consistent Schrödinger equation:

$$\left(-\frac{\hbar^2}{2m}\nabla^2 + \mu_{xc}([n];\vec{r}) + \phi([n];\vec{r}) + \delta v(\vec{r}) \right) \psi_i(\vec{r}) = \epsilon_i \psi_i(\vec{r}) , \tag{2.6}$$

where $\mu_{xc}([n];\vec{r}) = \delta E_{xc}/\delta n(\vec{r})$ is the exchange-correlation potential. Equation (2.6) is a consequence of the variational principle,[10] which says that $E[n]$ is minimal for the true electron density with respect to all variations of $n(\vec{r})$ at fixed $N = \int d\vec{r}\, n(\vec{r})$.

The exchange and correlation energy $E_{xc}[n]$ is not known exactly, and must in practice be replaced by some approximation, e.g., the local density approximation[11] (LDA), for which the rigorous proof of the minimal property of $E[n]$ is lost. However, the LDA is known[9,11] to give an excellent approximation to $n(\vec{r})$ and a good approximation to $E[n]$, which can be systematically improved by e.g., the method of wave-vector analysis.[7-9]

Before applying (2.3) to the metal surface problem, we review its application to bulk metals. With the choice $n_+(\vec{r}) = \bar{n}$, where $\bar{n}$ is the bulk average of $n(\vec{r})$, the large-parentheses term of (2.3) becomes simply the Madelung energy $N\epsilon_M$ of a neutralized lattice (see Appendix B). The bulk binding energy per electron $\epsilon = E[n]/N$ then becomes:

$$\epsilon = \epsilon_s(\bar{n}) + \epsilon_{xc}(\bar{n}) + \bar{w}_R + \epsilon_M + \epsilon_{bs} , \tag{2.7}$$

where ϵ_s and ϵ_{xc} are the kinetic and exchange-correlation contributions for an assumed *uniform* electron density $n(\vec{r}) = \bar{n}$, and all the nonuniformity of the real $n(\vec{r})$ is contained in the band-structure contribution ϵ_{bs} (see Appendix C). Expressions for the individual terms in (2.7) have been given by Ashcroft and Langreth[41]; in Table II we present results for 9 simple metals obtained from the Ashcroft pseudopotential,[42] for which $w_R(r)$ cancels $-ze^2/r$ exactly within a distance r_c from the nucleus

$$w_R(r) = \frac{ze^2}{r}\Theta(r_c - r) . \tag{2.8}$$

Here, as in our surface calculations, we have used the same input parameters (for the $\bar{n}$, z, r_c, and Wigner[43] parametrization of ϵ_{xc}, see Table III) as those of Lang and Kohn.[2]

Examination of Table II leads to several conclusions that we will rely on in our treatment of the *surface*:

(i) The band-structure contribution to the bulk binding energy is a small fraction of the total, and is typically less than half an eV; this supports our picture of the bulk as a region of essentially uniform electron density. (ii) Except for Li and Zn, where the pseudopotential is apparently in error,

TABLE III. Input parameters for the bulk and surface calculations of this paper (from Refs. 2 and 41). z is the valence, r_s the bulk density parameter ($\frac{4}{3}\pi r_s^3 = \bar{n}^{-1}$), and r_c the pseudopotential core radius. For r_s in a.u., the Wigner parametrization (Ref. 43) of ϵ_{xc} is

$$\epsilon_{xc}(\bar{n}) = \frac{-12.46}{r_s} - \frac{11.97}{r_s + 7.8}\ \frac{\text{eV}}{\text{electron}}$$

Metal	z	(a.u.) r_s	r_c
Al	3	2.07	1.12
Pb	4	2.30	1.12
Zn	2	2.30	1.27
Mg	2	2.65	1.39
Li	1	3.28	1.06
Na	1	3.99	1.67
K	1	4.96	2.14
Rb	1	5.23	2.61
Cs	1	5.63	2.93

the theoretical binding energies agree with the experimental ones within about 0.4 eV. The first-order pseudopotential contribution to ϵ

$$\bar{w}_R = \frac{\bar{n}}{z}\int d\vec{r}\, w_R(r) = 2\pi e^2 \bar{n} r_c^2 \tag{2.9}$$

is substantial. We conclude that $\bar{w}_R$ is given rather accurately (within about 0.4 eV) by the Ashcroft potential for all the simple metals except Li and Zn. This has an important bearing on the physical reality of our surface results—it means that the error in our parameter $\langle \delta v \rangle_{av}$ is probably less than 0.4 eV for all the metals except Li and Zn. We thought it important to check this point explicitly, since the Ashcroft r_c was fitted to experiment at or near the first nonzero reciprocal lattice vector $\vec{G}$, while $\bar{w}_R$ is inherently a part of the $G=0$ Fourier coefficient of the potential.

In fairness, we ought to point out that there is still a problem with the Ashcroft potential: Ashcroft and Langreth[41] found that the energy functional (2.3) using the Ashcroft potential did not minimize at exactly the observed equilibrium bulk density $\bar{n}$ for most of the bulk metals (Al is a notable exception). In order to make it do so, and so calculate the compressibility, they treated the $G=0$ Fourier coefficient of w_R as an adjustable parameter. This procedure, besides being inapplicable to the surface problem, tends to somewhat worsen the binding energies for most of the metals. Perhaps the real problem with the Ashcroft potential is that when the *a priori* nonlocal pseudopotential is approximated by a local pseudopotential, the parameter (s) of the local pseudopotential should depend somewhat on the bulk density $\bar{n}$.[44] Since the Ashcroft parameter r_c was fitted to experiment at the observed equilibrium bulk density $\bar{n}$, the Ashcroft potential should be more suitable for calculating properties at the observed equilibrium $\bar{n}$ (such as the bulk binding energy and the surface energy) than for calculating properties related to changes in $\bar{n}$. At any rate we provisionally accept the unmodified Ashcroft pseudopotential (2.8) as a suitable one for treating the metal surface, in order to make a meaningful comparison of our results with those of Lang and Kohn.[2,5] Note however that because of the problem described above, this pseudopotential probably should not be used to calculate relaxation of the positions of the first lattice planes at the surface (except for Al—see Appendix E).

III. SURFACE ENERGY: VARIATIONAL FORMULATION

We turn now from the infinite metal to the semi-infinite one filling the half space $x<0$, for which it is convenient to take

$$n_+(\vec{r}) = \bar{n}\Theta(-x)\,. \tag{3.1}$$

TABLE IV. The distance between lattice planes d, as a fraction of r_0, the radius of the Wigner-Seitz sphericalized cell ($\frac{4}{3}\pi r_0^3 = z/\bar{n}$). (Zn, $c/a = 1.861$; Mg, $c/a = 1.625$ (Ref. 54).

fcc	$\frac{d}{r_0}$	bcc	$\frac{d}{r_0}$
(111)	1.4774	(110)	1.4361
(100)	1.2794	(100)	1.0155
(110)	0.9047	(111)	0.5863
hcp		$\frac{d}{r_0}$	
(0001)		$1.4774[(c/a)/1.6330]^{2/3}$	

The surface energy is of course the piece of (2.3) that is proportional to the surface area. With the choice (3.1), the jellium model is described by just the first three terms of (2.3). Lang and Kohn[2] solved this model exactly (within the LDA) for $n(x)$, and then used *this* $n(x)$ to evaluate the fourth term in (2.3)—i.e., they treated $\delta v(\vec{r})$ as a first-order perturbation. (The distance along the x-direction between lattice planes is given in Table IV.) Results of the Lang-Kohn perturbational-self-consistent approach are shown in Tables V and VI.

We now appeal to the variational principle as discussed in Sec. II, i.e.,

$$\delta E[n]|_N = 0\,, \tag{3.2}$$

where the variation of $n(\vec{r})$ is taken at fixed electron number $N = \int d\vec{r}\, n(\vec{r})$. We obtain the surface energy by minimizing $E[n]$, Eq. (2.3), over a class of one-dimensional density profiles $n(x)$ which, like the jellium model profile, tend to $\bar{n}$ as x tends to $-\infty$. Unless $\delta v(\vec{r})$ is truly weak, it should be possible to find members of this class which give significantly lower energies than does the jellium-model profile. Since the bulk density $\bar{n}$ is held

TABLE V. Work function W^{jel} (Eq. 4.7) and its components for the *jellium model* [$\delta v(\vec{r})=0$] of the metal surface. The Fermi level phase shift $\gamma^{jel}(k_F)$ is also shown for this model.

Metal	D_e^{jel}	(eV) $\epsilon_F(\bar{n})$	$\mu_{xc}(\bar{n})$	W^{jel}	$\gamma^{jel}(k_F) - \frac{1}{4}\pi$
Al	6.24	11.69	−9.32	3.88	0.90
Pb	4.77	9.47	−8.50	3.80	0.81
Zn	4.77	9.47	−8.50	3.80	0.81
Mg	3.29	7.13	−7.51	3.67	0.71
Li	1.81	4.66	−6.25	3.40	0.58
Na	0.96	3.15	−5.29	3.10	0.48
K	0.36	2.04	−4.41	2.73	0.41
Rb	0.26	1.83	−4.22	2.65	0.37
Cs	0.14	1.58	−3.97	2.53	0.34

TABLE VI. Face-dependent surface energies calculated by the *perturbational self-consistent* method in the local density approximation (LDA).

Metal	Face	σ^{LDA} (ergs/cm^2)	Metal	Face	σ^{LDA} (ergs/cm^2)
Al fcc	(111)	730	Na bcc	(110)	229
	(100)	1485		(100)	262
	(110)	3230		(111)	351
Pb fcc	(111)	1140	K bcc	(110)	139
	(100)	2280		(100)	159
	(110)	4940		(111)	207
Zn hcp	(0001)	482	Rb bcc	(110)	122
Mg hcp	(0001)	546		(100)	115
				(111)	149
Li bcc	(110)	375	Cs bcc	(110)	103
	(100)	503		(100)	92
	(111)	685		(111)	116

fixed at the experimental value during the variation, it is only necessary to minimize the surface energy σ, which can be written in the LDA as

$$\sigma^{\mathrm{LDA}}[n] = \sigma_s[n] + \sigma_{xc}^{\mathrm{LDA}}[n] + \sigma_{\mathrm{es}}[n] + \sigma_{\mathrm{ps}}[n] + \sigma_R + \sigma_{\mathrm{cl}}, \tag{3.3}$$

where these six terms correspond in order to the surface pieces of the six terms in (2.3). The last two terms in (3.3) arise in the classical cleavage step described by Lang and Kohn, in which the crystal is cleaved sharply along a plane with the electron density inside each semi-infinite crystal held fixed at its bulk value (which is taken here to be the constant $\bar{n}$), and the first four terms in (3.3) arise in the subsequent relaxation of the electron density profile.

Lang and Kohn[2] have already given expressions for the functional dependence of the first four terms in (3.3) on the profile $n(x)$, and for the profile-independent classical cleavage energy σ_{cl}. We only write down two of these terms which are of particular interest here: the exchange-correlation contribution in the LDA

$$\sigma_{xc}^{\mathrm{LDA}}[n] = \int_{-\infty}^{\infty} dx\,[n(x)\epsilon_{xc}(n(x)) - \bar{n}\epsilon_{xc}(\bar{n})\Theta(-x)] \tag{3.4}$$

and the pseudopotential contribution

$$\sigma_{\mathrm{ps}}[n] = \int_{-\infty}^{\infty} dx\,\delta v(x)[n(x) - \bar{n}\Theta(-x)], \tag{3.5}$$

where $\delta v(x)$ is the average of $\delta v(\vec{r})$ over a plane at x parallel to the surface. [$\delta v(x)$ is displayed for Pb(111) and Cs(110) in Figs. 1 and 2 of this paper, and for K(110) in Fig. 6 of Ref. 2. The explicit expression for $\delta v(x)$ is given in Ref. 2 and also in our Appendix D.] A quantity of particular interest is the average value of $\delta v(\vec{r})$ over the volume of the semi-infinite crystal

$$\langle \delta v \rangle_{\mathrm{av}} = \frac{1}{d}\int_{-2d}^{-d} dx\,\delta v(x) = \bar{w}_R - \pi e^2 \bar{n} \tfrac{1}{6} d^2 \tag{3.6}$$

(see Table I), where d is the distance between neighboring lattice planes parallel to the surface (see Table IV). In the absence of lattice relaxation (not considered here—but see Appendix E), the first lattice plane is at $x = -\frac{1}{2}d$. σ_R in Eq. (3.3) is a profile-independent term in the surface energy,

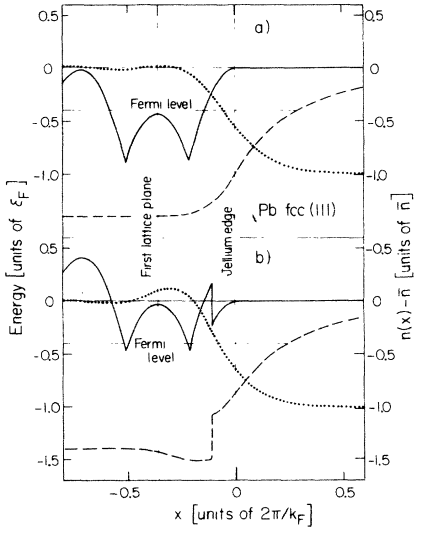

FIG. 1. Elements of the perturbational self-consistent (a) and variational self-consistent (b) schemes for the (111) face of fcc Pb. Dotted curve: electron density $n(x)$. Dashed curve: self-consistent one-electron potential which generates $n(x)$. Solid curve: planar average of the residual perturbation, which is $\delta v(x)$ in case (a) and $\delta v(x) - \langle \delta v \rangle_{\mathrm{av}}\,\theta(-x + X_m)$ in case (b). [Variational form (3.10). We have chosen $\phi([n]; +\infty) = 0$.]

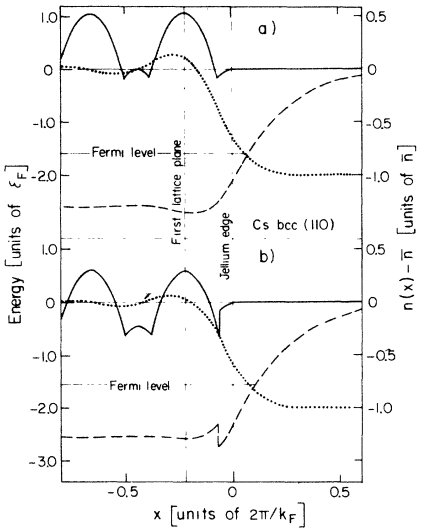

FIG. 2. Elements of the perturbational self-consistent (a) and variational self-consistent (b) schemes for the (110) face of bcc Cs. (See caption of Fig. 1).

$$\sigma_R = -\pi e^2 \bar{n}^2 d\,(r_c - \tfrac{1}{2}d)^2 \Theta(r_c - \tfrac{1}{2}d) \tag{3.7}$$

which arises only in the case $r_c > \frac{1}{2}d$ (see Appendix D); this case did not arise for the most densely packed faces considered by Lang and Kohn.[2]

Now it is only necessary to select the exact class of profiles $n(x)$ over which $\sigma[n]$ is to be minimized. One approach which has been applied both to jellium[12] and to real metals,[38,39] is to parametrize $n(x)$ directly. This approach, which has the advantage of simplicity, also has several major disadvantages—$T_s[n]$ cannot be evaluated exactly, no information is gained about the one-electron wave functions, and the approach is not readily applicable to other problems such as chemisorption. Another approach, which we take here, is to parametrize the effective potential[36,37,45] that appears in the Schrödinger equation (2.6) and generates the variational wave functions from which $n(x)$ and $T_s[n]$ can be constructed. In a purely-variational one-dimensional approach, the entire effective potential would be replaced by a parametrized function of x. But in the *variational self-consistent* approach of this paper, only $\delta v(\vec{r})$ is replaced by a parametrized function $V(x)$, i.e., the variational wave functions are generated from the self-consistent solution of the equation

$$\left(-\frac{\hbar^2}{2m}\nabla^2 + \mu_{xc}(n(x)) + \phi([n];x) + V(x)\right)\psi_i(\vec{r}) = \epsilon_i \psi_i(\vec{r}) \tag{3.8}$$

which describes the jellium surface in the presence of a fictitious external potential $V(x)$.

Since a one-dimensional self-consistent problem must now be solved for each choice of $V(x)$, it is desirable that $V(x)$ should contain only one variational parameter. In addition we impose several physically motivated restrictions on $V(x)$: (a) $V(x)$ must tend to a constant potential as $x \to -\infty$ to insure that the bulk density is uniform; with this condition satisfied, (3.8) can be solved in the same way that Lang and Kohn[2] solved the jellium model [$V(x)=0$] problem (see also Appendix A). (b) $V(x)$ should tend to 0 as $x \to +\infty$ since $\delta v(\vec{r})$ also vanishes in this limit. (c) In order to allow for a clean separation of the total energy of the system into bulk and surface parts, $V(x)$ should not contain any structural information about $\delta v(\vec{r})$, since in the bulk metal the electron-density is taken to be uniform. (d) For some choice of variational parameter, $V(x)$ should be constant or zero in the region where the electron density is nonzero—thus the variational self-consistent approach is able to give an *exact* description of the jellium model of the surface, and does so in the appropriate limit $\delta v(\vec{r}) \to 0$.

Our original[1] choice for $V(x)$ was a step potential with the step at the nominal jellium edge:

$$V(x) = C\Theta(-x)\,. \tag{3.9}$$

When the variational parameter C is set to zero we recover the jellium model. Positive C pushes electrons out into the vacuum region, yielding a density profile that is more spread out and has a larger surface dipole moment than that of jellium, while negative C has the opposite effect. The *"best"* value C_m minimizes the surface energy $\sigma^{\mathrm{LDA}}[n]$. Since $\delta v(x)$ depends on the crystallographic cleavage plane, so necessarily does C_m.

We emphasize again that C is only a variational parameter that generates a class of density profiles. The energy functional that we minimize is the exact one (2.3) (within the LDA and the local pseudopotential approximation), which contains no explicit reference to C. Moreover by varying C we are varying only the surface piece of (2.3), since the bulk piece will be the same for all C. The exact real metal problem is formally recovered by introducing $\delta v(\vec{r}) - V(x)$ as a perturbation in (3.8); this perturbation hopefully has only a minimal effect on the density profile when $V(x) = C_m\Theta(-x)$.

We have found the not-unexpected result that C_m tends to mimic $\langle \delta v \rangle_{\mathrm{av}}$ (compare C_m from Table VII with $\langle \delta v \rangle_{\mathrm{av}}$ from Table I). In light of this we also tried a second variational form

$$V(x) = \langle \delta v \rangle_{\mathrm{av}} \Theta(-x + X) \tag{3.10}$$

in which the *position* X of the potential step is varied; typically the minimizing value X_m was

TABLE VII. Results of *variational self-consistent* calculations using the form (3.9). C_m is the minimizing value of the variational parameter, D_e the electronic relaxation dipole barrior, W the variational work function, $\gamma(k_F)$ the Fermi-level phase shift, and σ^{LDA} the LDA surface energy.

Metal	Face	C_m	D_e (eV)	W	$\gamma(k_F)-\frac{1}{4}\pi$	σ^{LDA} (erg/cm^2)
Al fcc	(111)	−1.9	4.7	4.0	0.8	643
	(100)	1.0	7.2	4.7	1.0	1460
	(110)	3.7	9.8	4.5	1.2	2870
Pb fcc	(111)	−6.3	0.8	3.7	0.4	550
	(100)	−2.6	2.9	3.8	0.6	2155
	(110)	1.9	6.5	4.4	1.0	4860
Zn hcp	(0001)	−0.4	4.5	4.2	0.8	478
Mg hcp	(0001)	0.4	3.7	4.2	0.8	541
Li bcc	(110)	−1.1	1.1	3.5	0.5	331
	(100)	0.3	2.0	3.4	0.6	501
	(111)	1.0	2.6	3.2	0.7	670
Na bcc	(110)	0.3	1.2	3.3	0.5	223
	(100)	1.1	1.8	3.0	0.6	245
	(111)	1.5	2.1	2.7	0.7	321
K bcc	(110)	0.4	0.7	2.9	0.4	135
	(100)	1.1	1.2	2.7	0.6	147
	(111)	1.4	1.4	2.5	0.6	187
Rb bcc	(110)	1.1	1.1	2.9	0.6	110
	(100)	1.6	1.5	2.6	0.7	91
	(111)	1.8	1.7	2.3	0.7	118
Cs bcc	(110)	1.3	1.1	2.8	0.6	85
	(100)	1.5	1.3	2.3	0.6	68
	(111)	1.7	1.5	2.2	0.7	89

TABLE VIII. Results of *variational self-consistent* calculations using the form (3.10) (see caption of Table VII). X_m is the minimizing value of the variational parameter.

Metal	Face	$-2X_m/d$	D_e (eV)	W	$\gamma(k_F)-\frac{1}{4}\pi$	σ^{LDA} (erg/cm^2)
Al fcc	(111)	0.0	4.8	4.1	0.8	643
	(100)	0.5	6.4	3.9	0.9	1465
	(110)	0.1	9.1	3.8	1.1	2870
Pb fcc	(111)	0.3	0.9	3.9	0.5	365
	(100)	0.1	3.1	4.0	0.7	2150
	(110)	0.2	5.9	3.8	0.9	4865
Li bcc	(110)	0.2	1.1	3.6	0.5	358
Na bcc	(110)	0.5	1.0	3.1	0.5	228
	(100)	0.1	1.7	2.9	0.6	245
	(111)	0.0	2.1	2.8	0.7	321
K bcc	(110)	0.4	0.5	2.7	0.4	138
Rb bcc	(110)	0.3	0.8	2.6	0.5	108
Cs bcc	(110)	0.3	0.8	2.5	0.5	85
	(111)	0.0	1.5	2.2	0.7	89

TABLE IX. The surface energy σ and the exchange-correlation ($\sigma_{xc} = \sigma_{xc}^{LDA} + \Delta\sigma_{xc}$) and pseudopotential ($\sigma_{ps}$) contributions to it for the most densely packed faces of nine simple metals. For each metal surface the first horizontal line gives the *perturbational self-consistent* value and the second one gives the *variational self-consistent* value. (Here the variational principle has been invoked to choose between the forms (3.9) and (3.10): The values shown correspond in each case to the lower value of σ^{LDA} obtained from the two forms.) For a more complete breakdown of the surface energy of Pb and Cs into individual components, see Ref. 1.

Metal	Face	σ_{xc}^{LDA}	$\Delta\sigma_{xc}$ (erg/cm^2)	σ_{ps}	σ
Al fcc	(111)	2870	155	1050	885
		2545	150	900	795
Pb fcc	(111)	1965	112	935	1255
		1305	91	−280	456
Zn hcp	(0001)	1965	112	568	594
		1900	112	561	590
Mg hcp	(0001)	1175	72	290	620
		1230	73	285	619
Li bcc	(110)	540	37	110	412
		450	34	80	392
Na bcc	(110)	263	20	36	249
		280	20	34	247
K bcc	(110)	116	10	23	149
		133	11	19	148
Rb bcc	(110)	94	8	20	130
		122	9	1	117
Cs bcc	(110)	71	6	20	109
		100	8	−6	93

found somewhere between the nominal jellium edge $x=0$ and the first lattice plane $x=-\frac{1}{2}d$ (see Table VIII and Figs. 1 and 2). In fact for all the surfaces except Pb(111), good results can be obtained with $X=0$—physical insight alone almost allows us to dispense with the minimization procedure. The variational forms (3.9) and (3.10) usually gave closely similar results; we report the results of both forms to point out the power and also the limitations of the variational method.

We close this section by commenting on corrections to the local density approximation for exchange and correlation. We write

$$\sigma[n] = \sigma^{LDA}[n] + \Delta\sigma_{xc}[n], \tag{3.11}$$

where $\Delta\sigma_{xc}$ is the required correction, as given by the method of wave-vector analysis.[7-9] (We do not use the gradient expansion of $E_{xc}[n]$, which appears to be poorly convergent for physical density profiles.[9]) While $\Delta\sigma_{xc}[n]$ depends strongly on the bulk density $\bar{n}$, it is rather insensitive[9] (see Table IX) to the density profile. This means that the LDA gives a good density profile, and that $\Delta\sigma_{xc}[n]$ need not be included in the minimization of $\sigma[n]$—we simply minimize $\sigma^{LDA}[n]$ and then add on $\Delta\sigma_{xc}[n]$ evaluated[46] for the minimizing density profile.

IV. WORK FUNCTION AND DENSITY PROFILE

Lang and Kohn[5] have shown that the exact work function corresponding to the energy functional (2.1) is (in our notation[40])

$$W[n] = \phi([n]; x=+\infty) - \bar{\mu}[n], \tag{4.1}$$

where the chemical potential μ is the volume average over the semi-infinite crystal of

$$\mu = \frac{\delta E}{\delta n(\vec{r})} = \frac{\delta(T_s + E_{xc})}{\delta n(\vec{r})} + \phi([n]; \vec{r}) + \delta v(\vec{r}) . \tag{4.2}$$

(4.1) is clearly a functional of $n(\vec{r})$, and if we replace the true $n(\vec{r})$ by our variational $n(x)$ we find

$$\bar{\phi} \to \phi([n]; x=-\infty) , \tag{4.3}$$

$$\frac{\delta(T_s + E_{xc})}{\delta n(\vec{r})} \to \frac{\partial}{\partial \bar{n}} \{\bar{n}[\epsilon_s(\bar{n}) + \epsilon_{xc}(\bar{n})]\}$$

$$= \epsilon_F(\bar{n}) + \mu_{xc}(\bar{n}) , \tag{4.4}$$

where $\epsilon_F(\bar{n}) = \hbar^2 k_F^2/2m$ and $\bar{n} = k_F^3/3\pi^2$. (Bulk band-structure contributions to $\bar{\mu}$, which are not in-

cluded in our variational scheme, are shown to be small in Table II). The *variational work function*[47] is therefore

$$W = D_e - [\epsilon_F(\bar{n}) + \mu_{xc}(\bar{n}) + \langle \delta v \rangle_{av}, \tag{4.5}$$

where

$$D_e = \phi([n]; +\infty) - \phi([n]; -\infty)$$
$$= 4\pi e^2 \int_{-\infty}^{\infty} dx\, x[n(x) - \bar{n}\Theta(-x)] \tag{4.6}$$

is the electronic-relaxation surface dipole barrier. Of course for the jellium model ($\delta v(\vec{r}) = 0$), Eqs. (4.1) and (4.5) both give the exact result

$$W^{jel} = D_e^{jel} - [\epsilon_F(\bar{n}) + \mu_{xc}(\bar{n})], \tag{4.7}$$

where D_e^{jel} is (4.6) evaluated for the jellium-model profile (see Table V).

For real metals (4.5) is an approximation, and the error in this approximation should reflect the error in the variational density profile, since $W[n]$ is not minimal with respect to variations of $n(\vec{r})$. Variationally derived values of D_e and W for real metals are presented in Tables VII and VIII. The variational form (3.10) has an extra element of self-consistency not found in (3.9): for (3.10) the exact work function for the model problem (3.8) [jellium surface plus external $V(x)$] is the same as the variational work function (4.5).

Note that while D_e is purely a surface contribution to W and $\epsilon_F + \mu_{xc}$ is purely a bulk contribution, $\langle \delta v \rangle_{av}$ contains both bulk and surface contributions, which can be separated in the following way: Divide the bulk metal into neutral Wigner-Seitz cells drawn around each ion. For one such cell, let $\delta v_{WS}(\vec{r})$ be the sum of the pseudopotential from the ion in this cell and the electrostatic potential of the uniform electronic density contained within it, with the convention that the $\delta v_{WS}(\vec{r})$ from this cell vanishes far outside it. Then write

$$\langle \delta v \rangle_{av} = \langle \delta v_{WS} \rangle_{av} - D_{cl}, \tag{4.8}$$

where $\langle \delta v_{WS} \rangle_{av}$ is the bulk contribution to $\langle \delta v \rangle_{av}$ and $-D_{cl}$ is the surface contribution. If the Wigner-Seitz cell is now approximated by a Wigner-Seitz sphere of radius r_0 (where $\frac{4}{3}\pi r_0^3 = z/\bar{n}$), we find

$$\delta v_{WS}(r) \approx \left(-\frac{ze^2}{r} + w_R(r) + \frac{3}{2}\frac{ze^2}{r_0} - \frac{ze^2 r^2}{2r_0^3} \right) \Theta(r_0 - r), \tag{4.9}$$

$$\langle \delta v_{WS} \rangle_{av} \approx \bar{w}_R - \frac{3ze^2}{10r_0}, \tag{4.10}$$

(see Table II)

$$D_{cl} \approx -\frac{3ze^2}{10r_0}\left[1 - \frac{5}{12}\left(\frac{d}{r_0}\right)^2\right]. \tag{4.11}$$

D_{cl} is the contribution to the surface dipole barrier that arises from the distortion of the Wigner-Seitz cells which occurs in the classical cleavage of Sec. III (see Appendix B), and D_e is the contribution that arises from the subsequent relaxation of the electron density. The variational work function (4.5) becomes

$$W = (D_e + D_{cl}) - [\epsilon_F(\bar{n}) + \mu_{xc}(\bar{n}) + \langle \delta v_{WS} \rangle_{av}], \tag{4.12}$$

where the first bracket is the surface contribution and the second is the bulk contribution, i.e., the chemical potential measured from the electrostatic potential at the edge of the sphericalized Wigner-Seitz cell, the electron density being taken as uniform and equal to $\bar{n}$. The "surface dipole barrier" defined by Heine and Hodges[48] corresponds to our $D_e + D_{cl}$ while that defined by Lang and Kohn[49] corresponds to our $D_e - \langle \delta v \rangle_{av} = D_e + D_{cl} - \langle \delta v_{WS} \rangle_{av}$. Note that in the atomic vacancy problem, the parameter that measures the deviation from the jellium model should be $\langle \delta v_{WS} \rangle_{av}$ and not $\langle \delta v \rangle_{av}$.

By (4.6), the electronic relaxation dipole barrier D_e is a convenient measure of the spread of the electron density profile at the surface. Another convenient measure of this spread is the Fermi-level phase shift $\gamma(k_F)$. Kenner and Allen[16] have shown that the surface contribution to the electronic density of states at the Fermi level is

$$\frac{m}{\hbar^2 \pi^2}\left(\gamma(k_F) - \frac{\pi}{4}\right) \tag{4.13}$$

(see Tables V, VII, and VIII). Both D_e and $\gamma(k_F)$ increase as the surface electron density profile becomes more spread out at fixed bulk density $\bar{n}$.

The variational density profile is

$$n(x) = \frac{1}{\pi^2}\int_0^{k_F} dk\, (k_F^2 - k^2)[\psi_k(x)]^2, \tag{4.14}$$

where due to the conditions imposed on the model potential $V(x)$

$$\psi_k(x) \to \sin[kx - \gamma(k)] \tag{4.15}$$

as $x \to -\infty$. Conservation of electron number

$$\int_{-\infty}^{\infty} dx[n(x) - \bar{n}\Theta(-x)] = 0 \tag{4.16}$$

implies the Sugiyama-Langreth phase-shift sum rule[14,15]

$$\frac{2}{k_F^2}\int_0^{k_F} dk\, k\gamma(k) = \frac{\pi}{4}. \tag{4.17}$$

The Budd-Vannimenus theorem[50] is easily generalized to the problem (3.8), where $V(x) = C\Theta(-x + X)$ (see Appendix F), with the result

$$\phi([n];0)-\phi([n];-\infty)$$
$$=\bar{n}\frac{\partial}{\partial\bar{n}}[\epsilon_s(\bar{n})+\epsilon_{xc}(\bar{n})]+C\frac{n(X)}{\bar{n}} \quad (4.18)$$

satisfied when a self-consistent solution is achieved.

V. DISCUSSION OF RESULTS AND CONCLUSIONS

Lang and Kohn[2] have suggested that the measured liquid metal surface tension extrapolated to zero absolute temperature for a given metal should be comparable to the surface energies calculated for the solid fcc (111) and bcc (110) faces. In Table X we make this comparison for the LDA and total surface energies calculated by the perturbational and variational self-consistent methods. The variational self-consistent values for $\sigma=\sigma^{\mathrm{LDA}}+\Delta\sigma_{xc}$ are in good agreement with experiment for all the metals except Li and Zn—for which the pseudopotential was shown to be inadequate for the *bulk* binding energy in Sec. II.

The perturbational self-consistent LDA values shown in Table X are almost the same as those found by Lang and Kohn,[2] and would be exactly the same except for two approximations used by them but not by us—they did their calculations only at half-integer values of $r_s=z^{-1/3}r_0$ and interpolated[51] between these values, and they ignored the small difference in $\delta v(x)$ between fcc (111) and bcc (110). It is clear from Tables IX and X that for *some* metal surfaces (see Al, Pb, and Cs) the variational self-consistent surface energies (either in the LDA or not) are significantly lower than the perturbational self-consistent values—for Pb fcc (111), there is a striking reduction of σ^{LDA} from 1255 to 365 erg/cm^2. Generally speaking, the perturbational self-consistent approach is only accurate when $\langle\delta v\rangle_{\mathrm{av}}$ is small compared to $\epsilon_F(\bar{n})$ and to the one-electron potential barrier of the jellium surface.

TABLE X. Comparison of calculated surface energies with measured liquid metal surface tensions σ^{exp} (from Ref. 2). The surface energy is $\sigma=\sigma^{\mathrm{LDA}}+\Delta\sigma_{xc}$. For each metal the first horizontal line gives the *perturbational self-consistent* value and the second one gives the *variational self-consistent* value (with the choice between forms (3.9) and (3.10) corresponding to the lower value of σ^{LDA}). In each case two calculated values are given in the form *a*–*b*: *a* is for an fcc (111) face and *b* for a bcc (110) face.

Metal	σ^{LDA}	σ (erg/cm^2)	σ^{exp}
Al	730-915	885-1070	1000
	643-870	795-1020	
Pb	1140-1400	1255-1510	620
	365-820	456-910	
Zn	341-410	453-522	300
	304-338	419-453	
Mg	544-612	616-684	720
	542-595	614-667	
Li	353-375	390-412	480
	330-358	364-392	
Na	223-229	243-249	230
	223-227	243-247	
K	136-139	146-149	150
	135-137	146-148	
Rb	122-122	130-130	120
	110-108	119-117	
Cs	104-103	110-109	90
	88-85	96-93	

While the correction $\Delta\sigma_{xc}$ to the LDA is only about 5 to 10% of $\sigma_{xc}^{\mathrm{LDA}}$ (see Table IX), it is often a larger (up to 25%—see Table X) contribution to the total σ. Since $\Delta\sigma_{xc}$ is positive, it tends to somewhat offset the lowering of the surface energy that was achieved variationally, so that the results of the Lang-Kohn perturbational calculation in the LDA are (partly because of this accident) rather close to our variational non-LDA results, with the single exception of Pb.

We have not evaluated $\Delta\sigma_{xc}$ for any faces other than the most densely packed ones. However since $\Delta\sigma_{xc}$ depends mainly on the bulk density $\bar{n}$ and is otherwise insensitive to the density profile, it can easily be estimated for the other faces from Table IX.

Surface energies calculated for the (111), (100), and (110) faces of the cubic metals and for the (0001) faces of the hexagonal metals are shown in Tables VII and VIII. The surface energies obtained by the different variational forms (3.9) and (3.10) are quite close for all the cases we have examined, with the single exception of Pb(111) where (3.10) is somewhat superior. Note the strong face dependence of the calculated surface energy for Al and Pb. While Al and Pb satisfy the claim of Lang and Kohn[2] (based on their perturbational self-consistent calculations) that the most densely packed face has the lowest energy, this claim is not satisfied for some of the alkali metals.

The variational work functions (Tables VII and VIII) obtained from the different variational forms (3.9) and (3.10) differ by as much as 0.7 eV—indicating a certain level of error in the variational density profiles of one or both forms (although the density profiles obtained from the two forms appear to the eye to be closely similar). A comparison of our computed work functions with experiment would therefore be a little premature. A

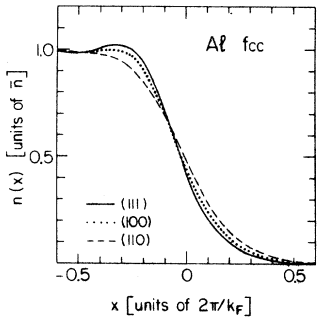

FIG. 3. Face-dependent electron density profiles for the surface of fcc Al [variational form (3.10)]. The profile for the (100) face is very close to the jellium-model profile.

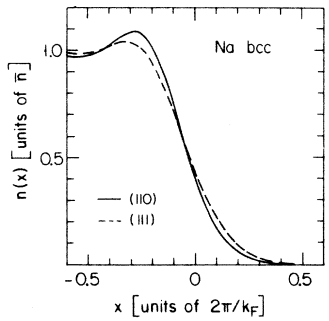

FIG. 5. Face-dependent electron density profiles for the surface of bcc Na [variational form (3.10)]. The profile for the (110) face is very close to the jellium-model profile. The (100) profile, not shown here, is close to the (111) profile.

better calculation of face-dependent work functions will be presented in a subsequent paper.[6]

Nevertheless the variational work functions argue strongly that our variational density profiles are much more realistic than those of the jellium model. Consider, for example, Al. If the density profile at the surface of Al were that of the jellium model, we could replace the electronic relaxation dipole barrier D_e by its jellium value $D_e^{\rm jel} = 6.2$ eV in the variational work function (4.5). Then the variational work function would be 5.5 eV for the (111) face and 0.9 eV for the (110) face of Al. This absurd result contradicts both experience and theory,[5] which agree that the work function should not vary from one face to another by more than a few tenths of an eV, and shows clearly that the density profiles at the surfaces of simple metals (at least in the absence of relaxation of the positions of the first lattice planes) are *not* jelliumlike and must in fact be strongly face dependent.

The strong face dependence of the variational density profile is shown in Figs. 3–6. It is also reflected in the face-dependence of D_e shown in Tables VII and VIII. Note that for a given metal the most densely packed face always has the tightest density profile with the smallest D_e and the largest Friedel oscillations—while the converse holds for the least densely packed face, for which the density profile is most spread out. All of these results could have been anticipated on the basis of the face dependence of $\langle \delta v \rangle_{\rm av}$ shown in Table I (and the change in $\langle \delta v \rangle_{\rm av}$ from one face to another is independent of the uncertain repulsive part w_R of the pseudopotential). While our variational values of D_e differ by as much as 5 eV from one face to another, our variational work functions [especially those obtained from the variational form (3.10)] differ from one face to another by only a few tenths of an eV, in qualitative agreement with theory[5] and experience. In fact we have shown that the principal effect of the discrete lattice perturbation $\delta v(\vec{r})$ on the electron density profile at the surface is to change D_e [Eq. (4.6)] in such a way that the variational work function (4.5) remains close to that of jellium. The principal mechanism for this effect is simply that $\delta v(\vec{r})$ has a nonzero average value $\langle \delta v \rangle_{\rm av}$ inside the metal and vanishes outside it.

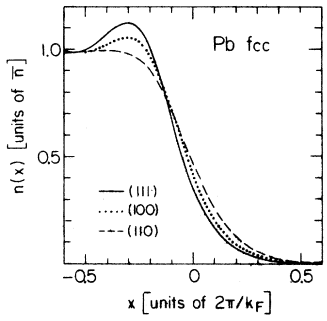

FIG. 4. Face-dependent electron density profiles for the surface of fcc Pb [variational form (3.10)]. The profile for the (110) face is closest to the jellium-model profile.

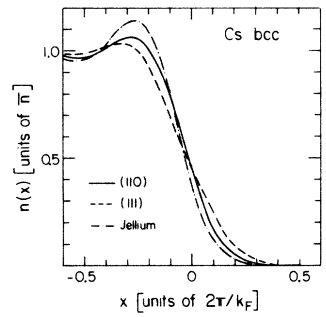

FIG. 6. Face-dependent electron density profiles for the surface of bcc Cs [variational form (3.10)]. The jellium-model profile is also shown.

In conclusion, we have presented a variational self-consistent generalization of the Lang-Kohn perturbational self-consistent approach to the metal surface, which retains most of the simplicity and utility of the latter. We have used this variational approach to calculate face-dependent surface energies, work functions and electron density profiles for nine simple metals. Calculated surface energies, including the correction to the local density approximation for exchange and correlation, are in satisfactory agreement with extrapolations to $T=0$ of measured surface tensions. Our results show that, while for many purposes the electron density can be regarded as uniform in the *bulk*, the surfaces of simple metals are rather unlike the surface of jellium—in particular the electron density profiles display a strong but easily understood and easily calculated face dependence.

Problems still to be explored include improvements in the pseudopotential, relaxation of the first lattice planes, and variation of the electron density over planes parallel to the surface; the latter two effects should only further reduce the calculated surface energies, and may reduce the strong anisotropy of the surface energy calculated here for Al and Pb. In Appendix E we argue that the electron density profile at the surface is strongly coupled (via $\langle \delta v \rangle_{av}$) to the relaxation of the first lattice plane. However the lattice relaxation we calculate there for the (111) face of fcc Al is negligible, so that our results for the electron density profile, work function, and energy of this surface remain essentially unchanged.

ACKNOWLEDGMENTS

It is a pleasure to thank David Langreth and John Wilkins for their continuing support and interest in this work, Norton Lang for helpful discussions and correspondence, Risto Nieminen for his efficient Lang-Kohn computer program, and G. Paasch[54] and J. R. Smith for helpful private communications.

APPENDIX A: SELF-CONSISTENCY PROCEDURE

The electrostatic potential (2.4) for one-dimensional density variation satisfies Poisson's equation

$$\frac{\partial^2 \phi}{\partial x^2} = -4\pi e^2 [n(x) - n_+(x)], \tag{A1}$$

which has the solution

$$\phi(x) = \phi(x_0) - \int_{x_0}^{x} dx' \int_{-\infty}^{x'} dx'' \, 4\pi e^2 [n(x'') - n_+(x'')]. \tag{A2}$$

But (A2) involves a double integration, and more importantly it causes instabilities in the iterative solution of the surface problem (3.8) due to the long-range of the Coulomb interaction: The Lang-Kohn[2] method requires matching at some $x_0 \ll 0$ of numerically integrated wave functions to bulk wave functions of the form (4.15), and so the region $x > x_0$ is not exactly charge neutral. After finding that straightforward iteration was unstable, Lang and Kohn devised a rather complicated method of solution which is described in their Appendix B.

An easier and more elegant method for solving (A1) has been given by Manninen, Nieminen, Hautojärvi, and Arponen.[20] However their solution is only valid in an infinite space $-\infty < x < +\infty$. Our numerical integration is always done in a finite space $x_0 < x < x_1$, and so we present here the needed generalization to this finite space. (We take $x_0 = -3.25(2\pi/k_F)$ and $x_1 = 1.5 \times (2\pi/k_F)$; x_0 is far enough inside the surface that the $O(x^{-2})$ terms in the potential (see Appendix A of Ref. 2) may be neglected, and x_1 is far enough outside the surface that $\phi(x)$ is essentially constant for all $x > x_1$.)

One can show by direct differentiation (see also Ref. 22) that Poisson's equation (A1) is satisfied for $x_0 < x < x_1$ if $\phi(x)$ satisfies the integral equation

$$\begin{aligned}\phi(x) = \frac{1}{2K} \int_{x_0}^{x_1} dx' \{ & 4\pi e^2 [n(x') - n_+(x')] \\ & + K^2 \phi(x') \} e^{-K|x-x'|} \\ & + \tfrac{1}{2} [\phi(x_0) - \phi'(x_0)/K] e^{-K(x-x_0)} \\ & + \tfrac{1}{2} [\phi(x_1) + \phi'(x_1)/K] e^{-K(x_1-x)},\end{aligned} \tag{A3}$$

where $\phi'(x) = d\phi/dx$ and K is an arbitrary constant. Aside from the boundary terms, this is just the equation of Manninen *et al.*[20]

Our procedure is to take $K \approx k_F$ and solve (A3) by iterating it to self-consistency along with (3.8), imposing the appropriate boundary conditions [in our case $\phi'(x_1) = 0$ and $\phi(x_0) =$ fixed constant] before each iteration by adjusting the coefficients of the boundary terms $e^{-K(x_1-x)}$ and $e^{-K(x-x_0)}$. (Note that for $K \gg k_F$ the convergence of the iteration is too slow, while for $K \ll k_F$ the instabilities associated with the long range of the Coulomb interaction reappear.) This procedure converges fastest when we have a reasonable first guess, within a few tenths of an eV, at the final value of $D_e = \phi(\infty) - \phi(-\infty)$ or equivalently of the variational work function W. The iterative procedure is straightforward—typically involving less than 50% feedback into the effective potential of (3.8) and full feedback into (A3), and converging to good simultaneous self-consistency of both equations after about 30 iterations, with all quantities well con-

verged and Eq. (4.17) and (4.18) well satisfied. The initial effective potential is a square barrier[45] with the barrier height adjusted to minimize the surface energy of the corresponding jellium, and the initial $\phi(x)$ is also a square barrier.

APPENDIX B: ELECTROSTATIC ENERGIES FOR $n(\vec{r}) = n_+(\vec{r})$

It is well known[52] that most of the Madelung energy of the bulk solid is accounted for by the electrostatic interactions *within* a neutral Wigner-Seitz sphere. Thus

$$\epsilon_M = -\eta z e^2/r_0 , \tag{B1}$$

where r_0 is the radius of the Wigner-Seitz sphere ($\frac{4}{3}\pi r_0^3 = z/\bar{n}$), and $\eta = 0.896$ for fcc, bcc, and ideal ($c/a = 1.633$) hcp structures.[41] (η depends only weakly on c/a: $\eta = 0.893$ for $c/a = 1.9$).[53] Evaluation of the electrostatic interaction within a single sphericalized cell gives $\eta = \frac{9}{10}$.

During the process of classical cleavage described in Sec. III, the Wigner-Seitz cells of the surface atoms are distorted (surface-flattened). It is reasonable to attribute nearly all of the classical cleavage energy

$$\sigma_{cl} = \alpha z e^2 \bar{n} \tag{B2}$$

to the electrostatic interactions between these distorted cells. Values of α for various faces and crystal structures are given in Ref. 2 and Ref. 54.

Now it is impossible to tell the difference between an fcc(111) cleavage and an ideal hcp (0001) cleavage by looking only at the first lattice planes on either side of the cleavage; it is only by looking at the *next* lattice plane on either side that one can tell the difference. Thus, we expect that to a good approximation

$$\alpha_{\text{ideal hcp}(0001)} \approx \alpha_{\text{fcc}(111)} . \tag{B3}$$

This surmise turns out to be correct[54] to within 3%.

The distortion of the Wigner-Seitz cells at the surface is also responsible for D_{cl}, Eq. (4.11), the classical cleavage contribution to the surface dipole barrier. D_{cl} is the same for fcc (111) and ideal hcp (0001) cleavages (see Table IV).

APPENDIX C: BAND-STRUCTURE CONTRIBUTIONS TO THE BINDING ENERGY AND CHEMICAL POTENTIAL

The band-structure contribution to the binding energy, Eq. (2.7), is[41]

$$\epsilon_{bs} = \frac{1}{2} \sum_{\vec{G}\neq 0} \frac{G^2}{4\pi e^2} \left(\frac{N_{ion}}{N}\right)^2 |w(G)|^2 \left(\frac{1}{\epsilon(G)} - 1\right) \bar{n} , \tag{C1}$$

where $\vec{G}$ is a reciprocal-lattice vector and

$$w(G) = \int d\vec{r}\, e^{-i\vec{G}\cdot\vec{r}} w(r) = -\frac{4\pi z e^2}{G^2} \cos(G r_c). \tag{C2}$$

$\epsilon(G)$ is the Lindhard dielectric function (we neglect the exchange-correlation contribution to ϵ_{bs}), and $N/N_{ion} = z$ for a neutral system.

The chemical potential (4.2) is

$$\bar{\mu} = \left.\frac{\partial E}{\partial N}\right|_{N_{ion}} , \tag{C3}$$

where the derivative with respect to electron number N is taken for a fixed number N_{ion} of ions at fixed positions, and the band-structure contribution to $\bar{\mu}$ is thus

$$\begin{aligned}\mu_{bs} &= \frac{\partial}{\partial \bar{n}} (\bar{n}\epsilon_{bs})\Big|_{N_{ion}} \\ &= -\frac{\bar{n}^2}{2z^2} \sum_{\vec{G}\neq 0} \frac{G^2}{4\pi e^2} |w(G)|^2 \frac{\partial}{\partial \bar{n}} \left(\frac{1}{\epsilon(G)} - 1\right) \\ &= \frac{-m\bar{n}^2}{2\hbar^2 k_F z^2} \sum_{\vec{G}\neq 0} \left|\frac{w(G)}{\epsilon(G)}\right|^2 \frac{1}{G} \ln\left|\frac{1+G/2k_F}{1-G/2k_F}\right| .\end{aligned} \tag{C4}$$

This is nothing else but the second-order correction[55] in $(\phi + \delta v)$ to the highest occupied eigenvalue

$$\bar{\mu} = \epsilon_F(\bar{n}) + \mu_{xc}(\bar{n}) + \bar{\phi} + \langle \delta v \rangle_{av} + \mu_{bs} \tag{C5}$$

of the one-electron Schrödinger equation (2.6) for the semi-infinite metal. Since $\bar{\mu}$ also appears in the exact work function (4.1), we have reached by an indirect route the conclusion that Koopmans' theorem is exact for a macroscopic metal; this conclusion can also be reached by more direct arguments.[56, 57]

Values of ϵ_{bs} and μ_{bs} calculated with the Ashcroft pseudopotential using only the first shell of nonzero reciprocal lattice vectors are shown in Table II. While it would not be consistent to include μ_{bs} in the variational work function (4.5), it is gratifying that μ_{bs} is never bigger than a few tenths of an eV.

APPENDIX D: THE CASE $r_c > \frac{1}{2}d$

Although Lang and Kohn[2] did not explicitly consider the case where the Ashcroft core radius r_c is greater than the distance $\frac{1}{2}d$ between the nominal jellium edge and the first lattice plane, the expressions in their Appendix D are readily adapted to it. This case arises for the bcc (111) faces of all the alkali metals and for the bcc (100) faces of Cs.

The planar average of $\delta v(\vec{r})$ is

$$\delta v(x) = \langle \delta v(\vec{r}) \rangle = \delta v_1(x) + \delta v_2(x) , \tag{D1}$$

where $\delta v_1(x)$ is given in Ref. (2):

$$\delta v_1(x) = \begin{cases} 0 ; & (0 \le x) , \\ u_1(x + ld) , & [-(l+1)d \le x \le -ld] , \end{cases} \tag{D2}$$

where $l = 0, 1, 2, 3 \ldots$ labels the lattice planes and

$$u_1(x) = -2\pi e^2 \bar{n} [x + d\theta(-x - \tfrac{1}{2} d)]^2 . \tag{D3}$$

Now

$$\delta v_2(x) = \left\langle \sum_{\vec{l}} w_R(|\vec{r} - \vec{l}|) \right\rangle = \sum_{l=0}^{\infty} u_2(x + ld) \tag{D4}$$

where

$$u_2(x) = 2\pi e^2 d\bar{n} (r_c - |x + \tfrac{1}{2} d|) \Theta(r_c - |x + \tfrac{1}{2} d|) . \tag{D5}$$

For $r_c < \frac{1}{2} d$,

$$\delta v_2(x) = \begin{cases} 0 , & (0 \le x) \\ u_2(x + ld) , & [-(l+1)d \le x \le -ld] . \end{cases} \tag{D6}$$

For $r_c > \frac{1}{2} d$ the terms in (D4) overlap. Thus for $\frac{3}{2} d > r_c > \frac{1}{2} d$, which covers all the remaining cases of interest here,

$$\delta v_2(x) = \begin{cases} 0 , & (r_c - \frac{1}{2} d) \le x) \\ u_2(x) + u_2(x + d) , & [-d \le x \le r_c - \tfrac{1}{2} d)] \\ u_2(x + ld) + u_2[x + (l-1)d] + u_2[x + (l+1)d] , & [-(l+1)d \le x \le -ld] , \end{cases} \tag{D7}$$

where $l = 1, 2, 3, \ldots$.

The new term in the surface energy is

$$\sigma_R = -\int_0^{\infty} dx \left\langle \sum_{\vec{l}} w_R(|\vec{r} - \vec{l}|) \right\rangle \bar{n}$$

$$= -\int_0^{\infty} dx \, \delta v_2(x) \bar{n} ; \tag{D8}$$

the result of the integration for $\frac{3}{2} d > r_c$ is (3.7). For all the surfaces considered in this paper, $|\sigma_R| \lesssim 50$ erg/cm^2.

APPENDIX E: RELAXATION OF THE FIRST LATTICE PLANE

Because of the problem with the pseudopotential discussed in Sec. II, we do not calculate here the relaxation of the position of the first lattice plane (except for Al). We give here mainly a *qualitative* discussion of the probable effect of such relaxation on the electron density profile and work function.

Consider a shift of the equilibrium position of the first lattice plane from $x = -\frac{1}{2} d$ to

$$x = (-\tfrac{1}{2} + \lambda) d . \tag{E1}$$

This shift gives rise to an extra contribution

$$-4\pi e^2 \bar{n} d^2 \lambda \tag{E2}$$

to the classical cleavage dipole barrier D_{el} [see Eq. (4.8)]. Consequently the volume average of the discrete lattice perturbation $\delta v(\vec{r})$ becomes

$$\langle \delta v(\lambda) \rangle_{av} = \bar{w}_R - \pi e^2 \bar{n} \tfrac{1}{6} d^2 (1 - 24\lambda) . \tag{E3}$$

Thus, an outward ($\lambda > 0$) shift of the first lattice plane by even a few percent of the bulk interplanar distance d can increase $\langle \delta v \rangle_{av}$ by as much as several eV. Our experience with $\langle \delta v \rangle_{av}$ for $\lambda = 0$ suggests that such a shift will increase the electronic relaxation dipole barrier D_e, and hence the spread of the electron density profile, in such a way that the variational work function (4.5) remains nearly constant. An inward shift of the first lattice plane will have the opposite effects.

Al is probably the only metal for which the Ashcroft pseudopotential is good enough to calculate lattice relaxation. Lang and Kohn[2] used the jellium profile to calculate $\lambda = +0.005$ for the (111) face of Al, with a corresponding reduction of 2% in σ^{LDA}. We have done a variational self-consistent calculation using our variational form (3.10), with the electron density profile at *each* λ chosen to minimize σ^{LDA}. We find $\lambda = +0.001$ with a corresponding reduction of less than 0.2% in σ^{LDA}. Our small outward relaxation of the first lattice plane shifts $\langle \delta v \rangle_{av}$ from -1.7 to -1.5 eV, with a corresponding spreading of the electron density profile—which is thus slightly more like jellium than the (111) profile shown in Fig. 3. In fact our calculated lattice relaxation is so small that it agrees essentially with a recent calculation by Tejedor and Flores,[58] who found no lattice relaxation in Al(111).

Since Lang and Kohn[2] gave the classical cleavage energy as a function of λ only for fcc (111), we cannot at present evaluate the lattice relaxation for the other faces of Al. We regard this as an interesting problem for future study.

APPENDIX F: PROOF OF THE GENERALIZED BUDD-VANNIMENUS THEOREM

The proof of (4.18), which closely follows the proof of the original ($C=0$) Budd-Vannimenus theorem,[50] will be outlined here. Consider a slab of jellium of macroscopic thickness L and area A, with periodic boundary conditions in the y and z directions:

$$n_+(x)=\bar{n}\Theta(-x)\Theta(x+L)\,, \tag{F1}$$

subject to an external potential

$$V(x)=C\Theta(-x+X)\Theta(x+L+X)\,, \tag{F2}$$

where X is some microscopic distance. The ground-state energy of this model system is

$$E[n_+,V,n]=T_s[n]+E_{xc}[n]+\frac{1}{2}\int d\vec{r}\,\phi([n];x)[n(x)-n_+(x)]+\int d\vec{r}\,V(x)n(x) \tag{F3}$$

with ϕ given by (2.4). (Other model energy functionals which generate (3.8) and resemble (2.3) more closely can be written down; since they all imply (4.18), we consider only the simplest one here.) Now consider an infinitesimal stretching of the whole system to new values.

$$L'=L+\Delta L\,, \tag{F4}$$

$$\bar{n}'=\bar{n}(1-\Delta L/L)=\bar{n}+\Delta\bar{n}\,, \tag{F5}$$

$$n'_+(x)=\bar{n}'\Theta(-x+\Delta L)\Theta(x+L)=n_+(x)+\Delta n_+(x)\,, \tag{F6}$$

$$V'(x)=C'\Theta(-x+X'+\Delta L)\Theta(x+L+X')=V(x)+\Delta V(x)\,, \tag{F7}$$

$$C'=C+\Delta\bar{n}\,\frac{\partial C}{\partial\bar{n}}\,, \tag{F8}$$

$$X'=X+\Delta\bar{n}\,\frac{\partial X}{\partial\bar{n}}\,. \tag{F9}$$

To first order in ΔL

$$E[n'_+,V',n']=E[n_+,V,n']-\int d\vec{r}\,\Delta n_+(x)\phi([n];x)+\int d\vec{r}\,n(x)\Delta V(x)\,. \tag{F10}$$

Now use the minimal property of E to find

$$\begin{aligned}\Delta E&=E[n'_+,V',n']-E[n_+,V,n]\\&=-\int d\vec{r}\,\Delta n_+(x)\phi([n];x)+\int d\vec{r}\,n(x)\Delta V(x)\\&=-\bar{n}A\,\Delta L\,\phi([n];0)+\bar{n}A\Delta L\,\phi([n];-\tfrac{1}{2}L)\\&\quad+CA\Delta Ln(X)+\bar{n}AL\,\Delta\bar{n}\,\frac{\partial C}{\partial\bar{n}}+o(\Delta L/L)\,.\end{aligned} \tag{F11}$$

But we can also write

$$E[n_+,V,n]=N[\epsilon_s(\bar{n})+\epsilon_{xc}(\bar{n})+C]+2A\sigma[n_+,V,n]\,, \tag{F12}$$

where $N=AL\bar{n}$ is the number of electrons. From (F12),

$$\Delta E=(AL\bar{n})\Delta\bar{n}\,\frac{\partial}{\partial\bar{n}}\,(\epsilon_s+\epsilon_{xc}+C)+o(\Delta L/L)\,. \tag{F13}$$

Equating (F11) and (F13) gives the desired result

$$\phi([n];0)-\phi([n];-\tfrac{1}{2}L)=\bar{n}\,\frac{\partial}{\partial\bar{n}}\,(\epsilon_s+\epsilon_{xc})+Cn(X)/\bar{n}\,. \tag{F14}$$

---

*Work supported in part by the Fonds National Suisse de la Recherche Scientifique.

†Present address: Laboratorium für Festkörperphysik, ETH, 8049 Zürich-Hönggerberg, Switzerland.

‡Work supported in part by the National Science Foundation under grant No. DMR 75-09804.

§Present address: Department of Physics, Tulane University, New Orleans, La. 70118.

[1]J. P. Perdew and R. Monnier, Phys. Rev. Lett. 37, 1286 (1976).
[2]N. D. Lang and W. Kohn, Phys. Rev. B 1, 4555 (1970).
[3]R. M. Nieminen, in Proceedings of the International Conference on Atomic Defects in Metals, Argonne, Illinois, 1976 (unpublished) and J. Nucl. Mater. (to be published).
[4]H. Hjelmberg, O. Gunnarsson, and B. I. Lundqvist (unpublished).
[5]N. D. Lang and W. Kohn, Phys. Rev. B 3, 1215 (1971).
[6]R. Monnier, J. P. Perdew, D. C. Langreth, and J. W. Wilkins (unpublished).
[7]D. C. Langreth and J. P. Perdew, Solid State Commun. 17, 1425 (1975).
[8]D. C. Langreth and J. P. Perdew, Phys. Rev. B 15, 2884 (1977).
[9]J. P. Perdew, D. C. Langreth, and V. Sahni, Phys. Rev. Lett. 38, 1030 (1977).
[10]P. Hohenberg and W. Kohn, Phys. Rev. 136, B864 (1964).
[11]W. Kohn and L. J. Sham, Phys. Rev. 140, A1333 (1965).
[12]J. R. Smith, Phys. Rev. 181, 522 (1969).
[13]A. J. Bennett and C. B. Duke, *Structure and Chemistry of Solid Surfaces*, edited by G. A. Somorjai (Wiley, New York, 1969).
[14]A. Sugiyama, J. Phys. Soc. Jpn. 15, 965 (1960).
[15]D. C. Langreth, Phys. Rev. B 5, 2842 (1972).
[16]V. E. Kenner and R. E. Allen, Phys. Rev. B 11, 2858 (1975).
[17]R. E. Allen, Solid State Commun. 16, 1143 (1975).

[18]R. L. Kautz and B. B. Schwartz, Phys. Rev. B 14, 2017 (1976).
[19]J. P. Perdew, Phys. Rev. B 16, 1525 (1977).
[20]M. Manninen, R. Nieminen, P. Hautojärvi, and J. Arponen, Phys. Rev. B 12, 4012 (1975).
[21]J. Ferrante and J. R. Smith, Solid State Commun. 20, 393 (1976).
[22]R. M. Nieminen, J. Phys. F 7, 375 (1977).
[23]Chemisorbed hydrogen: J. R. Smith, S. C. Ying, and W. Kohn, Phys. Rev. Lett. 30, 610 (1973) and Solid State Commun. 15, 1491 (1974); S. C. Ying, J. R. Smith, and W. Kohn, Phys. Rev. B 11, 1483 (1975); O. Gunnarsson and H. Hjelmberg, Phys. Scripta 11, 97 (1975); O. Gunnarsson, H. Hjelmberg, and B. I. Lundqvist, Phys. Rev. Lett. 37, 292 (1976).
[24]Chemisorbed H, Li, O, Cl, Si and Na: N. D. Lang and A. R. Williams, Phys. Rev. Lett. 34, 531 (1975) and Phys. Rev. Lett. 37, 212 (1976) and (unpublished).
[25]M. W. Finnis, J. Phys. F 5, 2227 (1975).
[26]E. Caruthers, L. Kleinman, and G. P. Alldredge, Phys. Rev. B 9, 3330 (1974).
[27]J. R. Chelikowsky, M. Schlüter, S. G. Louie, and M. L. Cohen, Solid State Commun. 17, 1103 (1975).
[28]E. Caruthers, L. Kleinman, and G. P. Alldredge, Phys. Rev. B 9, 3325 (1974).
[29]E. Caruthers, L. Kleinman, and G. P. Alldredge, Phys. Rev. B 8, 4570 (1973).
[30]R. W. Hardy and R. E. Allen, Solid State Commun. 19, 1 (1976), and Surface Science 61, 177 (1976).
[31]G. P. Alldredge and L. Kleinman, Phys. Rev. B 10, 559 (1974).
[32]J. A. Appelbaum and D. R. Hamann, Phys. Rev. B 6, 2166 (1972).
[33]J. H. Rose, Jr., H. B. Shore, D. J. W. Geldart, and M. Rasolt, Solid State Commun. 19, 619 (1976).
[34]K. H. Lau and W. Kohn, J. Phys. Chem. Solids 37, 99 (1976).
[35]A. K. Gupta and K. S. Singwi, Phys. Rev. B 15, 1801 (1977).
[36]J. H. Rose, Jr. and H. B. Shore, Solid State Commun. 17, 327 (1975).
[37]V. Sahni, J. B. Krieger, and J. Gruenebaum, Phys. Rev. B 15, 1941 (1977); V. Sahni, and J. Gruenebaum, Solid State Commun. 21, 463 (1977).
[38]G. Paasch and M. Hietschold, Phys. Status Solidi B 67, 743 (1975).
[39]M. Hietschold, G. Paasch, and P. Ziesche, Phys. Status Solidi B 70, 653 (1975).
[40]Note well that the potential denoted by ϕ in Ref. 5 is denoted by $\phi + \delta v$ here. Our notation $\bar{\mu}$ is also different from that of Ref. 5.
[41]N. W. Ashcroft and D. C. Langreth, Phys. Rev. 155, 682 (1967).
[42]N. W. Ashcroft, Phys. Lett. 23, 48 (1966).
[43]E. P. Wigner, Phys. Rev. 46, 1002 (1934). We use the corrected form given in Eq. (3.58) of D. Pines, *Elementary Excitations in Solids* (Benjamin, New York, 1963).
[44]J. P. Perdew and S. H. Vosko, J. Phys. F 6, 1421 (1976).
[45]G. D. Mahan, Phys. Rev. B 12, 5585 (1975).
[46]The method requires a decomposition of $\epsilon_{xc}(n)$ into contributions from density fluctuations of different wave vector K. Since this decomposition does not exist for the Wigner approximation, we have evaluated $\Delta\sigma_{xc}$ in the Hubbard approximation as in Ref. 8; closely similar values for $\Delta\sigma_{xc}$ would be obtained in, for example, the random-phase approximation, since $\Delta\sigma_{xc}$ arises mainly from the region of small K.
[47]This terminology is adopted for convenience. The variational work function is no sense a bound on the true work function.
[48]V. Heine and C. H. Hodges, J. Phys. C 5, 225 (1972).
[49]N. D. Lang and W. Kohn, Phys. Rev. B 8, 6010 (1973).
[50]H. F. Budd and J. Vannimenus, Phys. Rev. Lett. 31, 1218 and 1430(E) (1973); J. Vannimenus and H. F. Budd, Solid State Commun. 15, 1739 (1974).
[51]N. D. Lang (private communication). For the bulk density of Pb and Zn, $r_s = 2.30$, we find by actual calculation the value -184 erg/cm^2 for the surface energy of jellium, in contrast to the interpolated value -130 erg/cm^2 of Ref. 2.
[52]F. Seitz, *The Modern Theory of Solids* (McGraw-Hill, New York, 1940), p. 362.
[53]T. Schneider, Helv. Phys. Acta 42, 957 (1969).
[54]G. Paasch (private communication). Paasch has recalculated α for the cubic metals, and finds the same values as those of Ref. 2 except for the (111) face of the bcc crystal for which he finds $\alpha = 0.06295$. For hcp (0001) he finds $\alpha = 0.00327$ for the c/a ratio of Mg and 0.00162 for the c/a ratio of Zn. We have used Paasch's values of α in our calculations.
[55]T. Schneider, Phys. Status Solidi 32, 323 (1969).
[56]L. J. Sham and W. Kohn, Phys. Rev. 145, 561 (1965).
[57]F. K. Schulte, J. Phys. C 7, L370 (1974).
[58]C. Tejedor and F. Flores, J. Phys. F 6, 1647 (1976).